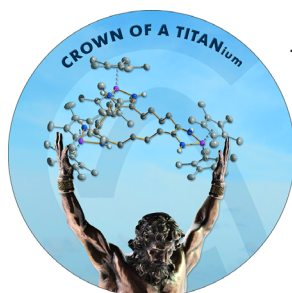


... offer exciting potential as activatable photosensitizers for photodynamic therapy. In their Communication on page 5340 ff., J. Yoon, E. U. Akkaya et al. report a photosensitizer that is switched on by a reaction with glutathione (GSH). Comparative cell culture data show that the agent is preferentially activated in cancer cells as they feature a higher glutathione level than normal cells.

Alloys

In their Communication on page 5312 ff., M. Saeys, A. N. Alexandrova, et al. present a chemical bonding model to explain the special stability and the reconstruction of surface cobalt and nickel carbides containing square-planar carbon atoms.

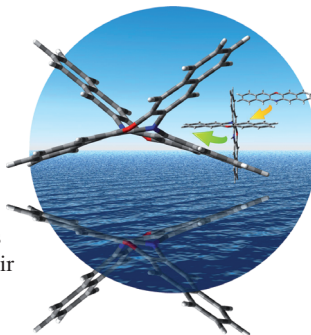


Titanacycles

U. Rosenthal et al. describe the formation of macrocycles from dinitriles and titanocenes in their Communication on page 5523 ff. The products are sometimes not stable and very difficult to characterize.

Helicenes

The synthesis of double N-hetero[5]helicenes that consist of two nitrogen-substituted heteropentacenes by tandem oxidative C–N couplings is described by D. Sakamaki, S. Seki, et al. in their Communication on page 5404 ff.



How to contact us:

Editorial Office:

E-mail: angewandte@wiley-vch.de

Fax: (+49) 62 01–606-331

Telephone: (+49) 62 01–606-315

Reprints, E-Prints, Posters, Calendars:

Carmen Leitner

E-mail: chem-reprints@wiley-vch.de

Fax: (+49) 62 01–606-331

Telephone: (+49) 62 01–606-327

Copyright Permission:

Bettina Loycke

E-mail: rights-and-licences@wiley-vch.de

Fax: (+49) 62 01–606-332

Telephone: (+49) 62 01–606-280

Online Open:

Margitta Schmitt, Carmen Leitner

E-mail: angewandte@wiley-vch.de

Fax: (+49) 62 01–606-331

Telephone: (+49) 62 01–606-315

Subscriptions:

www.wileycustomerhelp.com

Fax: (+49) 62 01–606-184

Telephone: 0800 1800536 (Germany only)
+44(0) 1865476721 (all other countries)

Advertising:

Marion Schulz

E-mail: mschulz@wiley-vch.de

jspiess@wiley-vch.de

Fax: (+49) 62 01–606-550

Telephone: (+49) 62 01–606-565

Courier Services:

Boschstrasse 12, 69469 Weinheim

Regular Mail:

Postfach 101161, 69451 Weinheim

Angewandte Chemie International Edition is a journal of the Gesellschaft Deutscher Chemiker (GDCh), the largest chemistry-related scientific society in continental Europe. Information on the various activities and services of the GDCh, for example, cheaper subscription to *Angewandte Chemie International Edition*, as well as applications for membership can be found at www.gdch.de or can be requested from GDCh, Postfach 900440, D-60444 Frankfurt am Main, Germany.

GDCh

GESELLSCHAFT
DEUTSCHER CHEMIKER

Get the **Angewandte App**
International Edition

Available on the
App Store

Enjoy Easy Browsing and a New Reading Experience on the iPad or iPhone

- Keep up to date with the latest articles in Early View.
- Download new weekly issues automatically when they are published.
- Read new or favorite articles anytime, anywhere.



Service

Spotlight on Angewandte's Sister Journals

5284 – 5287

Author Profile



*"If I could be anyone for a day, I would be an astronaut.
My favorite book is '1984' by George Orwell ..."*

This and more about Otto Dopfer can be found on page 5288.

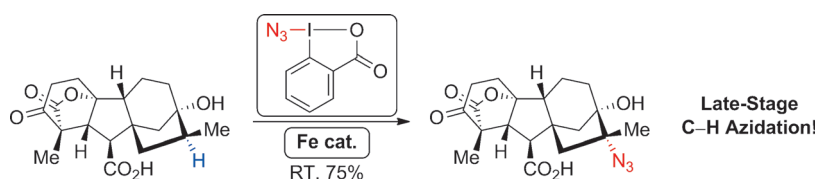
Otto Dopfer _____ 5288

Highlights

Azidation

M. V. Vita, J. Waser* _____ 5290 – 5292

Cyclic Hypervalent Iodine Reagents and
Iron Catalysts: The Winning Team for
Late-Stage C–H Azidation



1 + 1 = 3: By combining the exceptional reactivities of cyclic hypervalent iodine reagents and iron catalysts, Sharma and Hartwig achieved the azidation of C–H bonds with unprecedented efficiency and

selectivity. The late-stage introduction of azides into complex bioactive molecules will greatly facilitate the synthesis of analogues and accelerate the discovery of new chemical entities.

Reviews

Paper-Based Microfluidics

M. Eng. K. Yamada, T. G. Henares,
K. Suzuki, D. Citterio* — 5294–5310

Paper-Based Inkjet-Printed Microfluidic
Analytical Devices



Just inkjet it: Inkjet printing plays an important role as a process technology in the fast-growing field of microfluidic devices made of paper. This Review introduces the basics, strengths, and weaknesses related to the inkjet printing of functional materials essential for paper-based analytical devices. The discussion includes fundamental aspects as well as examples of analytical applications.

Communications



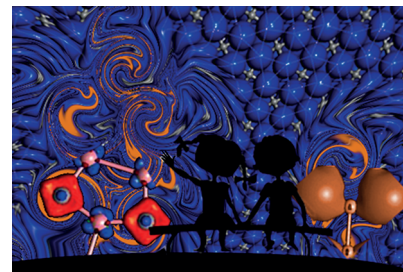
Alloys

A. Nandula, Q. T. Trinh, M. Saeys,*
A. N. Alexandrova* — 5312–5316



Origin of Extraordinary Stability of Square-Planar Carbon Atoms in Surface Carbides of Cobalt and Nickel

Out for the count: The unusual stability and reconstruction of surface cobalt and nickel carbides containing square-planar carbon atoms is explained by local aromaticity and electron count. A chemical bonding model for these systems is presented and explains the unusual structure, special stability, and the reconstruction. Several new aromatic and stable two-dimensional alloys are predicted.



Frontispiece

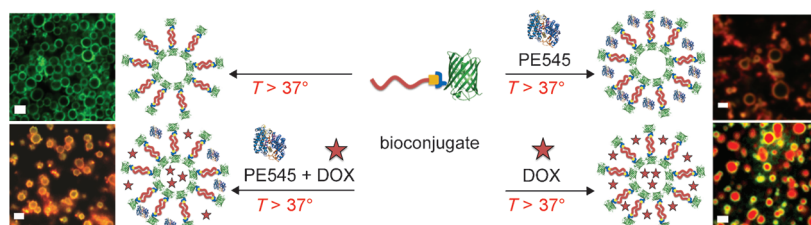


Polymersomes

C. K. Wong, A. J. Laos, A. H. Soeriyadi,
J. Wiedenmann, P. M. G. Curmi,
J. J. Gooding, C. P. Marquis,
M. H. Stenzel,
P. Thordarson* — 5317–5322



Polymersomes Prepared from Thermoresponsive Fluorescent Protein–Polymer Bioconjugates: Capture of and Report on Drug and Protein Payloads



Temperature-induced self-assembly: A temperature-sensitive green fluorescent (amilFP497) protein–polymer bioconjugate forms polymersomes above 37°C which encapsulate a mixture of pink

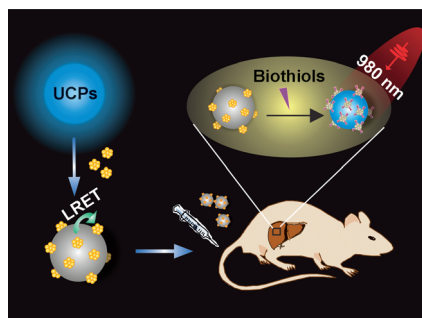
fluorescent protein (PE545) and a red drug molecule (DOX). The spatial location of the payload is revealed by fluorescence lifetime microscopy.

For the USA and Canada:

ANGEWANDTE CHEMIE International Edition (ISSN 1433-7851) is published weekly by Wiley-VCH, PO Box 191161, 69451 Weinheim, Germany. US mailing agent: SPP, PO Box 437, Emigsville, PA 17318. Periodicals postage

paid at Emigsville, PA. US POSTMASTER: send address changes to *Angewandte Chemie*, John Wiley & Sons Inc., C/O The Sheridan Press, PO Box 465, Hanover, PA 17331. Annual subscription price for institutions: US\$ 11.738/10.206 (valid for print and electronic / print or

electronic delivery); for individuals who are personal members of a national chemical society prices are available on request. Postage and handling charges included. All prices are subject to local VAT/sales tax.



Few but fine: A luminescence resonance energy transfer (LRET) probe for biothiols was constructed by decorating upconversion phosphors (UCPs) with dithiol-stabilized silver nanoclusters as energy acceptors. The probe was uploaded into living cells and used to detect intracellular biothiol levels with high discrimination. It was also found to be suitable for tissue imaging in vivo (see picture).

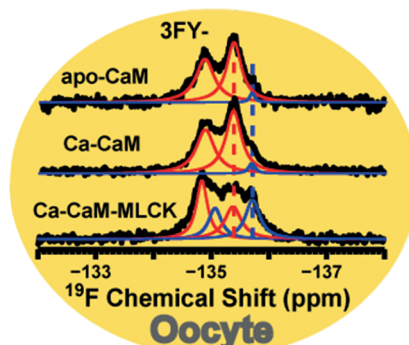
Biological Probes

Y. Xiao, L. Zeng, T. Xia, Z. Wu,
Z. Liu* 5323 – 5327

Construction of an Upconversion Nanoprobe with Few-Atom Silver Nanoclusters as the Energy Acceptor



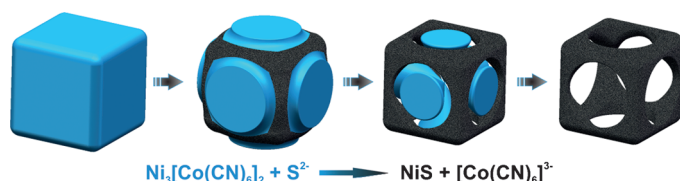
Confined in a cell: ^{19}F NMR spectroscopy has been used to directly observe transition between the free and Ca^{2+} -bound form of ^{19}F -labeled calmodulin (CaM) in intact *Xenopus* oocytes. Under physiological conditions, most CaM is in the apo form, and Ca-CaM only appears at high Ca^{2+} levels. The affinity of Ca^{2+} for CaM is enhanced by MLCK in cells. Paramagnetic NMR spectroscopy was also used to obtain long-range structural constraints.



In-Cell NMR Spectroscopy

Y. Ye, X. Liu, G. Xu, M. Liu,
C. Li* 5328 – 5330

Direct Observation of Ca^{2+} -Induced Calmodulin Conformational Transitions in Intact *Xenopus laevis* Oocytes by ^{19}F NMR Spectroscopy



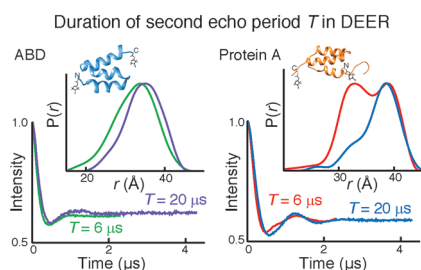
From frameworks to frames: Nickel sulfide nanoframes are synthesized through the reaction between Ni-Co Prussian blue analogue nanocubes and S^{2-} ions (see scheme). Benefitting from their structural

merits including open structure and high porosity, these NiS nanoframes exhibit enhanced electrochemical properties for both supercapacitors and hydrogen evolution reaction.

Nanostructures

X.-Y. Yu, L. Yu, H. B. Wu,
X. W. Lou* 5331 – 5335

Formation of Nickel Sulfide Nanoframes from Metal–Organic Frameworks with Enhanced Pseudocapacitive and Electrocatalytic Properties



Feel the pulse of the times: Pulsed double electron–electron resonance (DEER) is a powerful method in structural biology for obtaining $P(r)$ distance distributions between pairs of site-specific spin labels. However, the length of the second echo period can have a profound effect on DEER-derived $P(r)$ distributions (see graphs) owing to local environmental effects on spin-label phase memory relaxation times. It is shown how these effects can be minimized and circumvented.

Protein-Structure Elucidation

J. L. Baber,* J. M. Louis,
G. M. Clore* 5336 – 5339

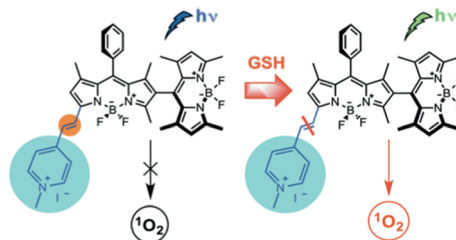
Dependence of Distance Distributions Derived from Double Electron–Electron Resonance Pulsed EPR Spectroscopy on Pulse-Sequence Time





Photodynamic Therapy

S. Kolemen, M. Işık, G. M. Kim, D. Kim,
H. Geng, M. Buyuktemiz, T. Karatas,
X.-F. Zhang, Y. Dede, J. Yoon,*
E. U. Akkaya* ————— 5340 – 5344



Selective switch: A dimeric BODIPY dye with reduced symmetry is ineffective as a photosensitizer unless it is activated by a reaction with intracellular glutathione (GSH). Staining with red-fluorescent

Annexin V shows that the photosensitizer is preferentially switched on in cancer cells, which feature a higher GSH level than normal cells.



Intracellular Modulation of Excited-State Dynamics in a Chromophore Dyad: Differential Enhancement of Photocytotoxicity Targeting Cancer Cells



Front Cover



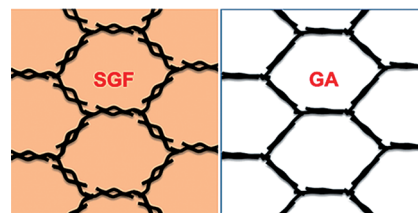
Lithium-Ion Batteries

Y. X. Xu, Z. Y. Lin, X. Zhong, B. Papandrea,
Y. Huang, X. F. Duan* ——— 5345 – 5350



Solvated Graphene Frameworks as High-Performance Anodes for Lithium-Ion Batteries

Solvated graphene frameworks (SGFs) that were prepared through a convenient solvent-exchange approach are binder-free anodes for lithium-ion batteries with significantly improved properties compared to unsolvated graphene frameworks. They exhibit ultrahigh reversible capacities, excellent rate capabilities, and superior cycling stabilities. GA = graphene aerogel.



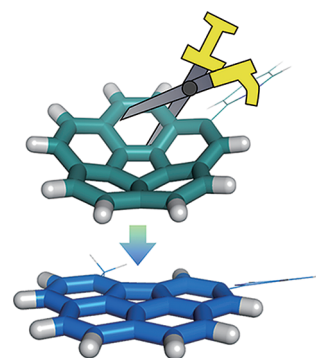
Corannulenes

S. Tashiro, M. Yamada,
M. Shionoya* ————— 5351 – 5354



Iridium-Catalyzed Reductive Carbon–Carbon Bond Cleavage Reaction on a Curved Pyridylcorannulene Skeleton

Iridium scissors: In the presence of a catalytic amount of $\text{IrCl}_3 \cdot n\text{H}_2\text{O}$ in ethylene glycol at 250 °C, 2-pyridylcorannulene undergoes a site-selective C–C bond cleavage reaction, which leads to a strain-free flat benzo[ghi]fluoranthene. This process is driven both by the coordination of the 2-pyridyl moiety to the iridium center and by strain relief of the curved corannulene skeleton.



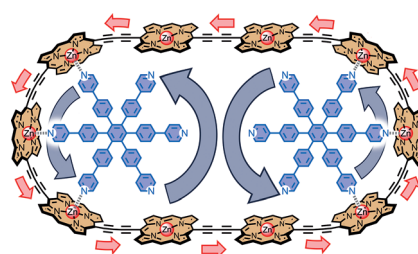
Molecular Gear

S. Liu, D. V. Kondratuk,
S. A. L. Rousseaux, G. Gil-Ramírez,
M. C. O'Sullivan, J. Cremers,
T. D. W. Claridge,
H. L. Anderson* ————— 5355 – 5359

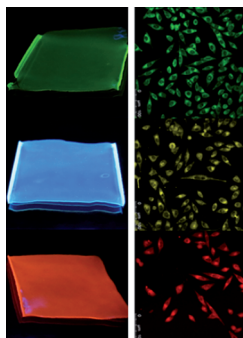


Caterpillar Track Complexes in Template-Directed Synthesis and Correlated Molecular Motion

Turning in unison: Two wheel-like templates work together to direct the synthesis of a nanoring. Their rotation is synchronized in the resulting 2:1 caterpillar track complex.



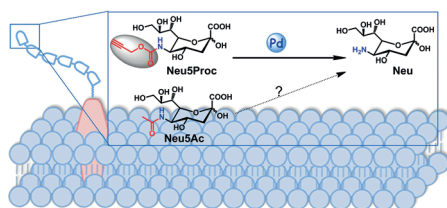
On the dot: A facile approach to photoluminescent carbon dots (CDs) that can be excited by a single wavelength and demonstrate emission of the three primary colors (red, green, and blue) is reported. The resulting CDs can be potentially used in the fabrication of flexible full-color emission films and in multicolor cellular imaging.



Carbon Dots

K. Jiang, S. Sun, L. Zhang, Y. Lu, A. Wu, C. Cai, H. Lin* — 5360–5363

Red, Green, and Blue Luminescence by Carbon Dots: Full-Color Emission Tuning and Multicolor Cellular Imaging



Chemical decaging: Palladium-mediated depropargylation (see scheme) was coupled with metabolic glycan labeling to mimic the enzymatic de-N-acetylation of Neu5Ac: a proposed mechanism for the natural occurrence of neuramic acid

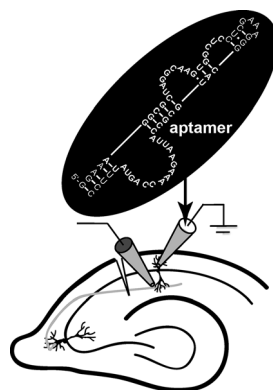
(Neu) on cell-surface glycans (Neu5Ac is N-acetylated Neu). Unmasking of the C5 amine by this strategy was used to manipulate cell-surface charge and neutralize the negatively charged carboxyl group of sialic acids.

Chemical Decaging

J. Wang, B. Cheng, J. Li, Z.-Y. Zhang, W.-Y. Hong, X. Chen,* P. R. Chen* — 5364–5368

Chemical Remodeling of Cell-Surface Sialic Acids through a Palladium-Triggered Bioorthogonal Elimination Reaction

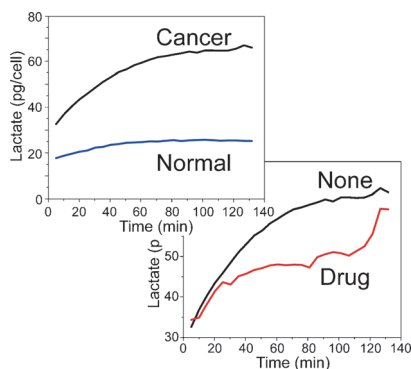
Clamp-it: Intracellular availability of functional aptamers is achievable through the patch-clamp pipette. The delivery of a specific aptamer in such a way leads to efficient inhibition of mitogen-activated kinase-dependent synaptic plasticity. This approach introduces synthetic aptamers as generic tools, readily applicable to study single components of intracellular signaling networks.



Neurosciences

S. Lennarz, T. C. Alich, T. Kelly, M. Blind, H. Beck, G. Mayer* — 5369–5373

Selective Aptamer-Based Control of Intraneuronal Signaling



Monitoring metabolism: For “In-cell NMR metabolomics”, live cells were harvested and centrifuged into an NMR tube. Using $^{13}\text{C}_6$ -glucose and heteronuclear NMR spectroscopy, real-time metabolic flux differences between cancer and normal cells were obtained. The method also detected live metabolic alteration by an anticancer agent, leading to the identification of new functional targets.

NMR Spectroscopy

H. Wen, Y. J. An, W. J. Xu, K. W. Kang, S. Park* — 5374–5377

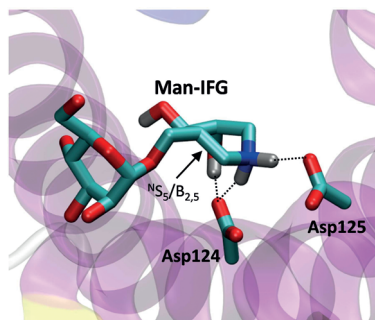
Real-Time Monitoring of Cancer Cell Metabolism and Effects of an Anticancer Agent using 2D In-Cell NMR Spectroscopy

Conformational Analysis

A. J. Thompson, G. Speciale,
J. Iglesias-Fernández, Z. Hakki, T. Belz,
A. Cartmell, R. J. Spears, E. Chandler,
M. J. Temple, J. Stepper, H. J. Gilbert,
C. Rovira,* S. J. Williams,*
G. J. Davies* _____ **5378–5382**



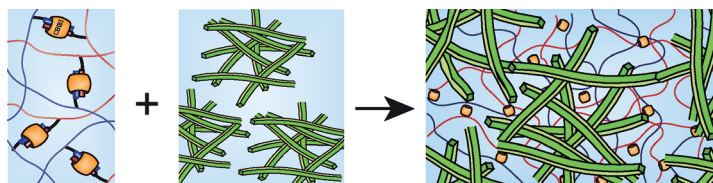
Evidence for a Boat Conformation at the
Transition State of GH76 α -1,6-
Mannanases—Key Enzymes in Bacterial
and Fungal Mannoprotein Metabolism



Family GH76 *endo*- α -mannanases participate in construction and breakdown of fungal cell wall mannoprotein. A combined synthetic, structural, and theoretical study discloses the first inhibitors of this family of enzymes and quantifies how the enzyme distorts an azasugar inhibitor into a transition-state-mimicking boat conformation.

Hydrogels

E.-R. Janeček, J. R. McKee, C. S. Y. Tan,
A. Nykänen, M. Kettunen, J. Laine,
O. Ikkala,*
O. A. Scherman* _____ **5383–5388**



Hybrid Supramolecular and Colloidal
Hydrogels that Bridge Multiple Length
Scales

The combination of a colloidal hydrogel consisting of nanofibrillated cellulose with an interpenetrating supramolecular hydrogel based on hydroxyethyl cellulose leads to a hybrid nanocomposite hydro-

gel. The two networks interact through hydroxyethyl cellulose adsorption to the nanofibrillated cellulose surfaces, resulting in an enhanced rheological yield strain and storage modulus.



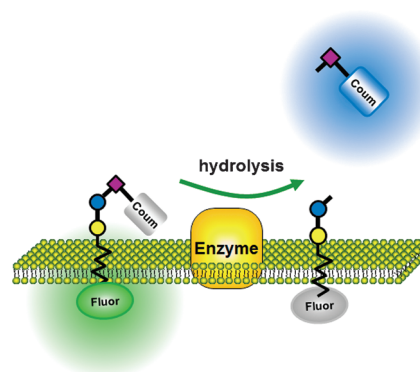
Fluorescent Probes

G. Y. Yang, C. Li, M. Fischer, C. W. Cairo,
Y. Feng, S. G. Withers* _____ **5389–5393**



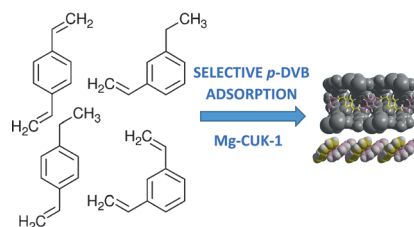
A FRET Probe for Cell-Based Imaging of
Ganglioside-Processing Enzyme Activity
and High-Throughput Screening

Clear-cut: A small-molecule FRET probe was designed and synthesized for monitoring at least three key enzymatic activities involved in ganglioside degradation. The substrate, which contains BODIPY (Fluor) and Coumarin (Coum) fluorophores at opposite termini, enables sensitive fluorogenic assay in both cell lysates and living cells and should be useful for dissecting the mechanisms of these enzymes, as well as for protein engineering and inhibitor development.



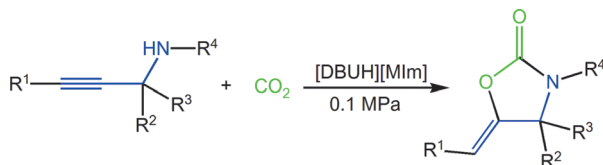
Para-Selective Liquid Sorption

B. Saccoccia, A. M. Bohnsack,
N. W. Waggoner, K. H. Cho, J. S. Lee,
D.-Y. Hong, V. M. Lynch, J.-S. Chang,*
S. M. Humphrey* _____ **5394–5398**



Separation of *p*-Divinylbenzene by
Selective Room-Temperature Adsorption
Inside Mg-CUK-1 Prepared by Aqueous
Microwave Synthesis

From complex to simple: The porous material Mg-CUK-1 has been prepared using an aqueous microwave-assisted synthetic method. This material contains infinite one-dimensional pores that show highly selective, room-temperature adsorption of *p*-divinylbenzene (*p*-DVB) and other organic compounds from complex mixtures of isomers.



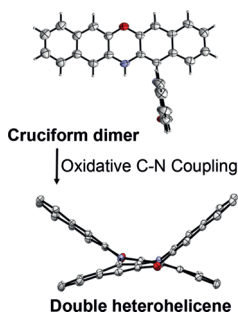
CO₂ capture: Under mild, metal-free conditions, protic ionic liquids, such as 1,8-diazabicyclo[5.4.0]-7-undecenium 2-methylimidazolid [DBUH][MIm], can catalyze the reaction between CO₂ and

propargylic amines to form 2-oxazolidinones. Both the cation and anion of the ionic liquids play key roles in accelerating the reaction.

Ionic Liquids

J. Hu, J. Ma,* Q. Zhu, Z. Zhang, C. Wu, B. Han* 5399–5403

Transformation of Atmospheric CO₂
Catalyzed by Protic Ionic Liquids: Efficient
Synthesis of 2-Oxazolidinones



Double N-hetero[5]helicenes that are composed of two nitrogen-substituted heteropentacenes were synthesized by tandem oxidative C–N couplings via the cruciform dimers in only two steps from commercially available naphthalene derivatives. These compounds are remarkably stable towards racemization, and the two heteroacenes moieties were shown to be strongly electronically coupled.

Helicenes

D. Sakamaki,* D. Kumano, E. Yashima, S. Seki* 5404–5407

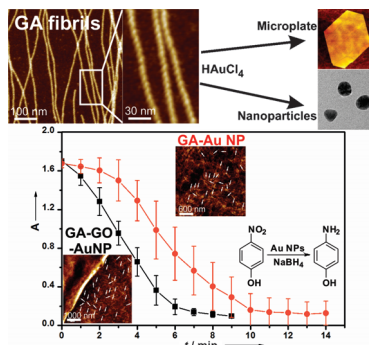
A Facile and Versatile Approach to Double
N-Heterohelicenes: Tandem Oxidative
C–N Couplings of N-Heteroacenes via
Cruciform Dimers



Back Cover



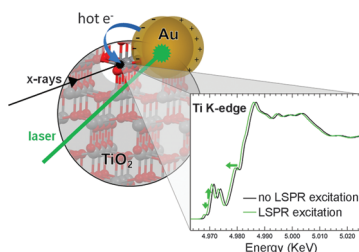
Hybrid nanomaterials: Self-assembled fibrillar networks of glycyrrhizic acid (GA) in water are used as scaffolds for the precision design of hybrid nanomaterials for use in catalysis. By incorporating graphene oxide and in situ synthesized gold nanoparticles, an enhanced catalytic efficiency is obtained as a result of the high affinity of the substrate to the graphene oxide.



Hydrogels

A. Saha, J. Adamcik, S. Bolisetty, S. Handschin, R. Mezzenga* 5408–5412

Fibrillar Networks of Glycyrrhizic Acid for
Hybrid Nanomaterials with Catalytic
Features



Hot electrons: An atomistic description of the electronic and structural changes of TiO₂ resulting from the injection of hot electrons is presented. High resolution X-ray spectroscopy shows that plasmonic charges are trapped on Ti states at the semiconductor surface, giving rise to transient low-coordinate Ti sites which have long-enough lifetimes to play a major role in catalytic processes (LSPR = localized surface plasmon resonance).

Plasmonic Photocatalysis

L. Amidani,* A. Naldoni,* M. Malvestuto, M. Marelli, P. Glatzel, V. Dal Santo, F. Boscherini 5413–5416

Probing Long-Lived Plasmonic-Generated
Charges in TiO₂/Au by High-Resolution
X-ray Absorption Spectroscopy



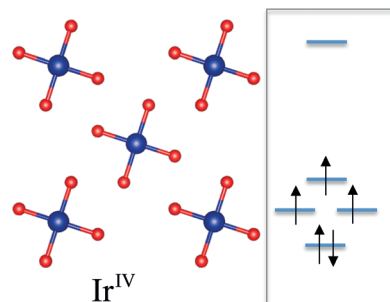
Coordination Geometry

S. Kanungo, B. Yan, P. Merz, C. Felser,
M. Jansen* — 5417 – 5420



Na_4IrO_4 : Square-Planar Coordination of a Transition Metal in d^5 Configuration due to Weak On-Site Coulomb Interactions

Bending the rules: A square-planar coordination mode in transition-metal (TM) complexes is typically assumed to require a d^8 or d^9 TM electronic configuration. A square-planar structure for the IrO_4 moiety in Na_4IrO_4 is reported where Ir^{IV} has a d^5 electronic configuration. The weak Coulomb interactions of Ir-5d states stabilize this unconventional square-planar structure.



Gas-Phase Chemistry

D. S. N. Parker, R. I. Kaiser,*
B. Bandyopadhyay, O. Kostko, T. P. Troy,
M. Ahmed* — 5421 – 5424



Unexpected Chemistry from the Reaction of Naphthyl and Acetylene at Combustion-Like Temperatures

Photoionization mass spectrometry was used to investigate the reaction of 1- and 2-naphthyl radicals in excess acetylene under combustion-like conditions. The reaction produces 1- and 2-ethynyl-naphthalenes (C_{12}H_8), acenaphthylene (C_{12}H_8); and diethynyl-naphthalenes (C_{14}H_8). Neither phenanthrene nor anthracene ($\text{C}_{14}\text{H}_{10}$) was found, which indicates that a hydrogen abstraction/acetylene addition mechanism does not lead to aromatic ring formation.

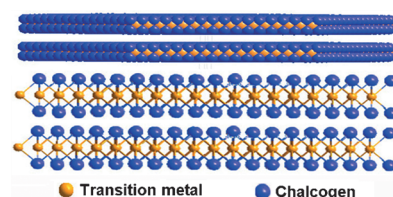


Nanostructures

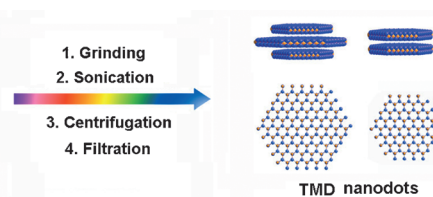
X. Zhang, Z. C. Lai, Z. D. Liu, C. L. Tan,
Y. Huang, B. Li, M. T. Zhao, L. H. Xie,
W. Huang, H. Zhang* — 5425 – 5428



A Facile and Universal Top-Down Method for Preparation of Monodisperse Transition-Metal Dichalcogenide Nanodots



On the dot: The title nanodots (NDs), including MoS_2 , WS_2 , ReS_2 , TaS_2 , MoSe_2 , WSe_2 , and NbSe_2 , are prepared from their bulk crystals by using a combination of grinding and sonication techniques. The



synthesized nanodots, mixed with polyvinylpyrrolidone, are used as active layers for fabrication of memory devices having a nonvolatile memory effect. TMD = transition-metal dichalcogenides.

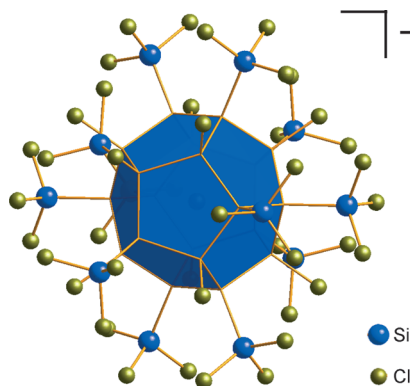


Silafullerenes

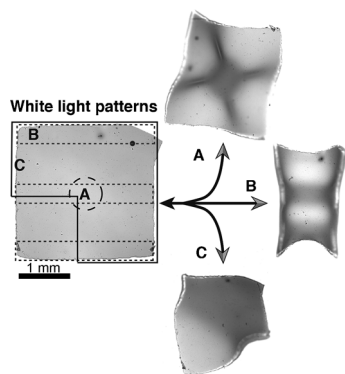
J. Tillmann, J. H. Wender, U. Bahr,
M. Bolte, H.-W. Lerner,
M. C. Holthausen,*
M. Wagner* — 5429 – 5433



One-Step Synthesis of a [20]Silafullerene with an Endohedral Chloride Ion



As simple as this: A stable, crystalline [20]silafullerene forms in preparatively useful yields through wet-chemical self-assembly from Si_2Cl_6 and chloride ions in the presence of an amine. Each silicon dodecahedron contains an endohedral chloride ion that imparts a net negative charge. Eight chloro substituents and twelve trichlorosilyl groups are attached to the surface of each cluster in a strictly regioregular arrangement.

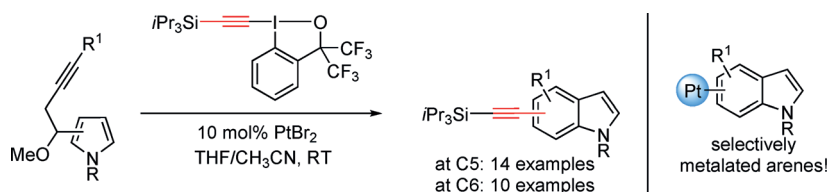


Re-programmable morphing: Patterns of white light are used to dynamically reconfigure photothermal nanocomposite hydrogel sheets into numerous 3D shapes. Fast and reversible transformations are achieved on timescales tuneable down to several seconds. This concept for externally adaptable elastic hydrogel sheets may find applications in soft robotics, drug delivery, or microfluidics.

Soft Matter

A. W. Hauser, A. A. Evans, J.-H. Na, R. C. Hayward* 5434–5437

Photothermally Reprogrammable Buckling of Nanocomposite Gel Sheets



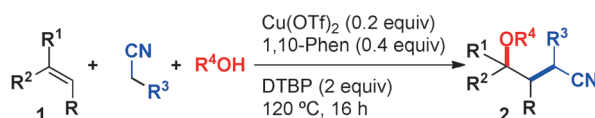
Pt and hyper-I: Indoles are omnipresent in natural products, bioactive molecules, and organic materials. To access benzene-ring-alkynylated indoles with an unsubstituted pyrrole ring is highly challenging. Reported here is the title reaction, which

selectively leads to C5- or C6-alkynylated indoles starting from easily available pyrroles. The ethynylbenziodoxole hyper-valent iodine reagent is key to the success of the reaction.

Heterocycle Synthesis

Y. Li, J. Waser* 5438–5442

Platinum-Catalyzed Domino Reaction with Benziodoxole Reagents for Accessing Benzene-Alkynylated Indoles



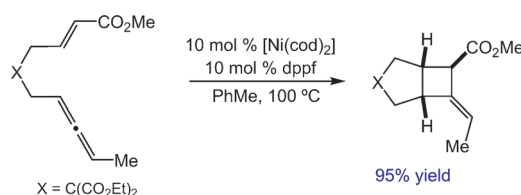
Three-component coupling of alkenes, alcohols, and alkyl nitriles catalyzed by copper triflate afforded 4-alkoxyalkyl nitriles in good to excellent yields. The reaction forms a C–C and a C–O bond

with concomitant creation of a quaternary carbon center. The involvement of a radical intermediate was proven by a radical clock experiment.

Synthetic Methods

C. Chatalova-Sazepin, Q. Wang, G. M. Sammis, J. Zhu* 5443–5446

Copper-Catalyzed Intermolecular Carboetherification of Unactivated Alkenes by Alkyl Nitriles and Alcohols



Nicked! The title reaction encompasses a broad range of ene-allene substrates, thus providing efficient access to fused cyclobutanes from easily accessed π -components. An inexpensive catalytic system comprised of $[\text{Ni}(\text{cod})_2]$ and dppf

was used, thus constituting an attractive approach to challenging cyclobutane frameworks under mild reaction conditions. cod = 1,5-cyclooctadiene, dppf = 1,1'-bis(diphenylphosphino)ferrocene.

Carbocycles

N. N. Noucti, E. J. Alexanian* 5447–5450

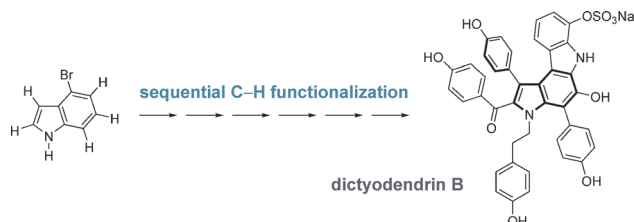
Stereoselective Nickel-Catalyzed [2+2] Cycloadditions of Ene-Allenes





Natural Product Synthesis

A. K. Pitts, F. O'Hara, R. H. Snell,
M. J. Gaunt* 5451 – 5455



A Concise and Scalable Strategy for the
Total Synthesis of Dictyodendrin B Based
on Sequential C–H Functionalization

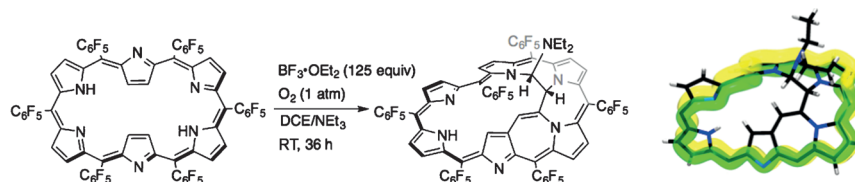
One by one: A sequential C–H functionalization strategy for the synthesis of the marine alkaloid dictyodendrin B is reported. The synthetic route begins from commercially available 4-bromoindole

and involves six direct functionalizations around the heteroarene core as part of a gram-scale strategy towards the natural product.



Porphyrinoids

T. Higashino, T. Soya, W. Kim, D. Kim,*
A. Osuka* 5456 – 5459



A Möbius Aromatic [28]Hexaphyrin
Bearing a Diethylamine Group: A Rigid
but Smooth Conjugation Circuit

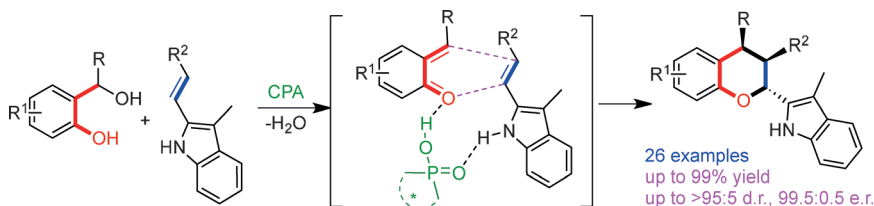
Möbius versus Hückel: An NEt₂-group-bearing [28]hexaphyrin was prepared from a [26]hexaphyrin (see Scheme) and is a rare example of a Möbius aromatic metal-free expanded porphyrin. It displays the largest diatropic ring current among

known [28]hexaphyrins. Reduction and oxidation of this molecule led to the production of a Hückel antiaromatic [28]hexaphyrin and a Hückel aromatic [26]hexaphyrin by a Möbius-to-Hückel topology switch.



Cycloaddition

J.-J. Zhao, S.-B. Sun, S.-H. He, Q. Wu,
F. Shi* 5460 – 5464



Catalytic Asymmetric Inverse-Electron-Demand Oxa-Diels–Alder Reaction of
In Situ Generated *ortho*-Quinone
Methides with 3-Methyl-2-Vinylindoles

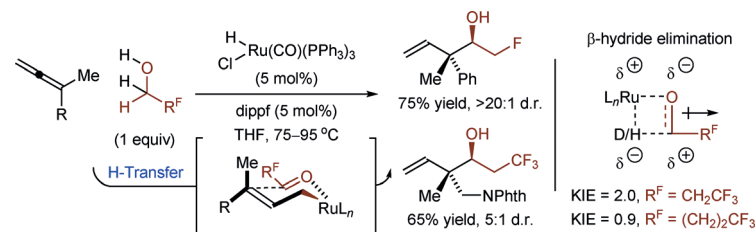
Three in a row: The title reaction of *ortho*-quinone methides, generated in situ from *ortho*-hydroxybenzyl alcohols, has been established. By selecting 3-methyl-2-vinylindoles as a class of competent dienophiles, this approach provides an efficient

strategy to construct enantioenriched chroman frameworks with three adjacent stereogenic centers in high yields and excellent stereoselectivities. CPA = chiral phosphoric acid.



Allylic Compounds

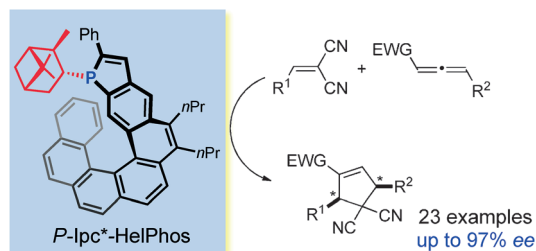
B. Sam, T. Luong,
M. J. Krische* 5465 – 5469



Ruthenium-Catalyzed C–C Coupling of
Fluorinated Alcohols with Allenes:
Dehydrogenation at the Energetic Limit of
 β -Hydride Elimination

Alcohol is the answer! Ruthenium(II) complexes catalyze the C–C coupling of 1,1-disubstituted allenes and fluorinated alcohols to form homoallylic alcohols bearing all-carbon quaternary centers with good to complete levels of diastereose-

lectivity. Whereas fluorinated alcohols are relatively abundant and tractable, the corresponding aldehydes are often not commercially available because of their instability.



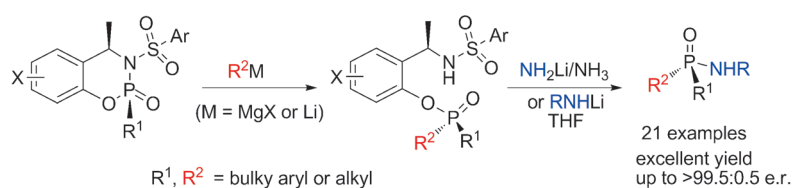
Helical P: Specially designed phosphahelicenes demonstrate high efficiency and enantioselectivity in organocatalytic cyclizations. These new helically chiral phos-

phines complement and outperform previous nucleophilic catalysts used in this field. lpc* = (1*R*,2*R*,3*R*,5*S*)-2,6,6-trimethylbicyclo[3.1.1]heptan-3-yl.

Asymmetric Catalysis

M. Gicquel, Y. Zhang, P. Aillard,
P. Retailleau, A. Voituriez,*
A. Marinetti* 5470–5473

Phosphahelicenes in Asymmetric Organocatalysis: [3+2] Cyclizations of γ -Substituted Allenes and Electron-Poor Olefins



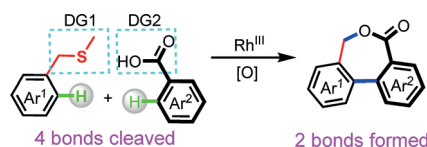
Making a 'Phos': A general, efficient, and highly enantioselective method for the synthesis of the title compounds relies on nucleophilic substitution of a chiral

phosphinate. These chiral phosphinamides were utilized for the synthesis of readily tunable P-stereogenic Lewis base organocatalysts.

Synthetic Methods

Z. S. Han,* L. Zhang, Y. Xu, J. D. Sieber,
M. A. Marsini, Z. Li, J. T. Reeves,
K. R. Fandrick, N. D. Patel,
J.-N. Desrosiers, B. Qu, A. Chen,
D. M. Rudzinski, L. P. Samankumara,
S. Ma, N. Grinberg, F. Roschangar,
N. K. Yee, G. Wang, J. J. Song,
C. H. Senanayake 5474–5477

Efficient Asymmetric Synthesis of Structurally Diverse P-Stereogenic Phosphinamides for Catalyst Design

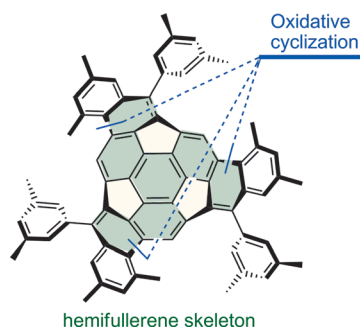


Double crossed! Reported is the rhodium(III)-catalyzed double C–H cross-coupling of benzyl thioethers and carboxylic acids. Two directing groups (DGs) are used to enhance the selectivity of the double C–H activation. One DG becomes part of the product and the other is removed in situ.

C–H Activation

X.-S. Zhang, Y.-F. Zhang, Z.-W. Li,
F.-X. Luo, Z.-J. Shi* 5478–5482

Synthesis of Dibenzo[*c,e*]oxepin-5(7*H*)-ones from Benzyl Thioethers and Carboxylic Acids: Rhodium-Catalyzed Double C–H Activation Controlled by Different Directing Groups



Bowl full of π : The two-step synthesis of a strained π bowl, having a hemifullerene skeleton from sumanene, was achieved in a high yield. The reaction involved a regioselective intramolecular oxidative cyclization as the key reaction. This cyclization is regioselective and is likely to be under thermodynamic control.

Fused-Ring Systems

T. Amaya,* T. Ito, T. Hirao* 5483–5487

Construction of a Hemifullerene Skeleton: A Regioselective Intramolecular Oxidative Cyclization



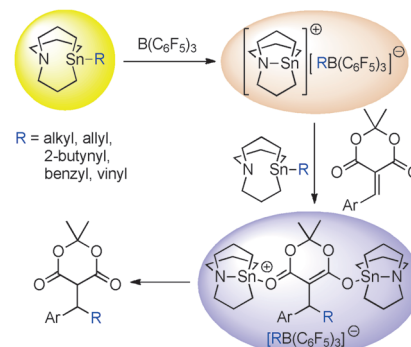
Alkylation

A. Kavooosi, E. Fillion* — 5488 – 5492



Synthesis and Characterization of Tricarbastannatranes and Their Reactivity in $B(C_6F_5)_3$ -Promoted Conjugate Additions

Trane of thought: Spectroscopic investigation on the structure of tricarbastannatranes has been carried out. The $B(C_6F_5)_3$ -promoted conjugate addition of alkyl-tricarbastannatranes to benzylidene derivatives of Meldrum's acid and detailed mechanistic studies are presented.



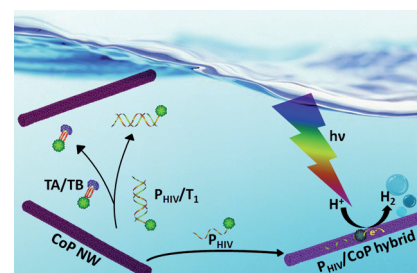
Nanostructures

J. Tian, N. Cheng, Q. Liu, W. Xing, X. Sun* — 5493 – 5497



Cobalt Phosphide Nanowires: Efficient Nanostructures for Fluorescence Sensing of Biomolecules and Photocatalytic Evolution of Dihydrogen from Water under Visible Light

Quenched: The high fluorescence quenching ability of cobalt phosphide nanowires (CoP NWs) and their different affinity toward single-stranded and double-stranded DNA were used to develop a rapid fluorescence assay for nucleic acids and proteins. The attachment of dye-labelled oligonucleotide probes to the surface of the CoP semiconductor leads to greatly enhanced photocatalytic hydrogen evolution from H_2O under visible light.



B,N Heterocycles

D.-T. Yang, S. K. Møllerup, X. Wang, J.-S. Lu, S. Wang* — 5498 – 5501



Reversible 1,1-Hydroboration: Boryl Insertion into a C–N Bond and Competitive Elimination of HBR_2 or R–H



NBC news: Boranes (HBR_2) have been found to undergo facile and unprecedented 1,1-hydroboration with pyrido[1,2-a]isoindole (A) via an intermediate D, generating a variety of BN heterocycles

(B) that can either undergo thermal retro-hydroboration or R–H elimination producing brightly fluorescent BN-phenanthrenes (C).

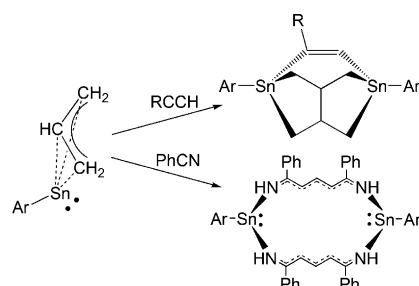
Inside Cover

Allyl Tin Complexes

K. M. Krebs, J. Wiederkehr, J. Schneider, H. Schubert, K. Eichele, L. Wesemann* — 5502 – 5506

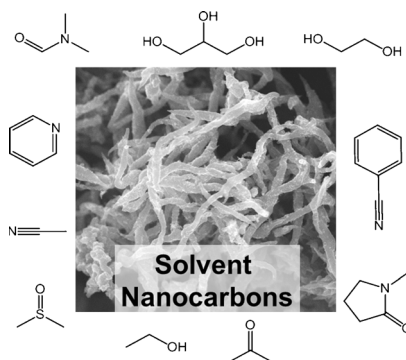


η^3 -Allyl Coordination at Tin(II)—Reactivity towards Alkynes and Benzonitrile



3 to II: An example for the η^3 coordination of an allyl group to a Sn^{II} center is presented. The allyl tin(II) compound undergoes allyl couplings in reactions with alkynes to yield tricyclic systems, and a sixteen-membered macrocycle is formed with benzonitrile (see Scheme).

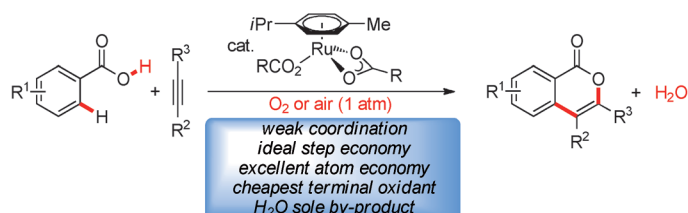
Hot stuff: Hot-injection techniques were combined with ionothermal chemistry to transform common organic solvents into nanostructured porous carbons with high yields. The same method can be further applied to synthesize various carbon/inorganic composites, for example, for electrocatalytic applications.



Nanostructures

Y. Chang, M. Antonietti,
T.-P. Fellerger* 5507–5512

Synthesis of Nanostructured Carbon through Ionothermal Carbonization of Common Organic Solvents and Solutions



C–H Activation

S. Warratz, C. Kornhaas, A. Cajaraville,
B. Niepötter, D. Stalke,
L. Ackermann* 5513–5517

Ruthenium(II)-Catalyzed C–H Activation/
Alkyne Annulation by Weak Coordination
with O2 as the Sole Oxidant



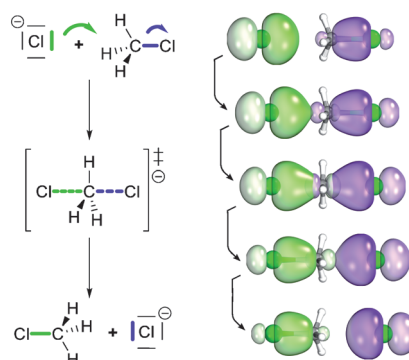
Air and water: Ruthenium(II) biscarboxylates allow for the annulation of alkynes and alkenes by oxidative C–H functionalizations with molecular oxygen as the sole

oxidant. The C–H/O–H functionalization process occurs with excellent selectivities under mild reaction conditions, with water produced as the only by-product.

Curly arrows from ab initio calculations:

Curly arrows in reaction mechanisms are shown to correspond to changes in intrinsic bond orbitals (IBOs) along reaction paths. With this quantum chemical basis, even complex reaction mechanisms can be derived and visualized in a simple, direct, and intuitive form.

Empirical Mechanism ↔ Intrinsic Bond Orbitals



Reaction Mechanisms

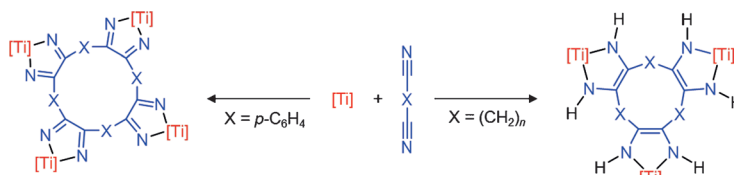
G. Knizia,* J. E. M. N. Klein 5518–5522

Electron Flow in Reaction Mechanisms—
Revealed from First Principles



Metallacycles

L. Becker, P. Arndt, A. Spannenberg,
H. Jiao, U. Rosenthal* — 5523 – 5526



Big and beautiful: The reaction of $[\text{Cp}^*_2\text{Ti}]$ with dicyano compounds led to macro-molecules through nitrile–nitrile C–C couplings. Depending on the bridging unit X, the size and type of the macrocycle varies between three- and four-membered

1-metalla-2,5-diaza-cyclopenta-2,4-dienes (left) and a 1-metalla-2,5-diaza-cyclopent-3-ene (right). The structures of the products were investigated by X-ray crystallography and DFT analysis.

Inside Back Cover



Supporting information is available on www.angewandte.org (see article for access details).



A video clip is available as Supporting Information on www.angewandte.org (see article for access details).



This article is available online free of charge (Open Access).



This article is accompanied by a cover picture (front or back cover, and inside or outside).



The Very Important Papers, marked VIP, have been rated unanimously as very important by the referees.

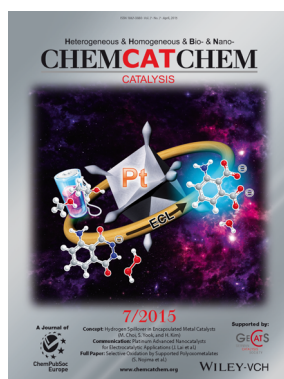


The Hot Papers are articles that the Editors have chosen on the basis of the referee reports to be of particular importance for an intensely studied area of research.

Check out these journals:



www.chemasianj.org



www.chemcatchem.org



www.chempluschem.org



www.chemviews.org

Angewandte Corrigendum

On page 11507 of this Communication, the last sentence of the left column must read: "The intensity increase from stage 1 to stage 4 is consistent with a distorted octahedral coordination environment of high-spin Fe^{III} in Fh in stage 2 and the presence of tetrahedral Fe^{III} in magnetite in stage 4.^[14b]"

During copy-editing, mistakes were accidentally introduced in the numbering of the stages in Figures 2 and 3. The editorial staff apologizes for this mishap. Corrected versions of both figures are shown here.

Selective Formation of Metastable Ferrihydrite in the Chiton Tooth

L. M. Gordon, J. K. Román, R. M. Everly,
M. J. Cohen, J. J. Wilker,
D. Joester* 11506–11509

Angew. Chem. Int. Ed. 2014, 53

DOI: 10.1002/anie.201406131

